

Article

Induction of Apoptosis, Autophagy and Ferroptosis by *Thymus vulgaris* and *Arctium lappa* Extract in Leukemia and Multiple Myeloma Cell Lines

Aveen N. Adham^{1,2}, Mohamed Elamir F. Hegazy^{2,3} , Alaadin M. Naqishbandi^{1,*}  and Thomas Efferth^{2,*}

¹ Department of Pharmacognosy, College of Pharmacy, Hawler Medical University, Erbil 44001, Kurdistan Region, Iraq; aveen.adham@hmu.edu.krd

² Department of Pharmaceutical Biology, Institute of Pharmaceutical and Biomedical Sciences, Johannes Gutenberg University, Staudinger Weg 5, 55128 Mainz, Germany; mohegazy@uni-mainz.de

³ Chemistry of Medicinal Plants Department, National Research Centre, 33 El-Bohouth St., Dokki, Giza 12622, Egypt

* Correspondence: alaadin.naqishbandi@hmu.edu.krd (A.M.N.); efferth@uni-mainz.de (T.E.); Tel.: +964-75-0448-2788 (A.M.N.); +49-6131-3925751 (T.E.)

Academic Editor: Roberto Fabiani

Received: 24 September 2020; Accepted: 28 October 2020; Published: 29 October 2020



Abstract: *Thymus vulgaris* and *Arctium lappa* have been used as a folk remedy in the Iraqi Kurdistan region to deal with different health problems. The aim of the current study is to investigate the cytotoxicity of *T. vulgaris* and *A. lappa* in leukemia and multiple myeloma (MM) cell lines and determine the mode of cell death triggered by the most potent cytotoxic fractions of both plants in MM. Resazurin assay was used to evaluate cytotoxic and ferroptosis activity, apoptosis, and modulation in the cell cycle phase were investigated via Annexin V-FITC/PI dual stain and cell-cycle arrest assays. Furthermore, we used western blotting assay for the determination of autophagy cell death. *n*-Hexane, chloroform, ethyl acetate, and butanol fractions of *T. vulgaris* and *A. lappa* exhibited cytotoxicity in CCRF-CEM and CEM/ADR 5000 cell lines at concentration range 0.001–100 µg/mL with potential activity revealed by chloroform and ethyl acetate fractions. NCI-H929 displayed pronounced sensitivity towards *T. vulgaris* (TCF) and *A. lappa* (ACF) chloroform fractions with IC₅₀ values of 6.49 ± 1.48 and 21.9 ± 0.69 µg/mL, respectively. TCF induced apoptosis in NCI-H929 cells with a higher ratio (71%), compared to ACF (50%) at 4 × IC₅₀. ACF demonstrated more potent autophagy activity than TCF. TCF and ACF induced cell cycle arrest and ferroptosis. Apigenin and nobiletin were identified in TCF, while nobiletin, ursolic acid, and lupeol were the main compounds identified in ACF. *T. vulgaris* and *A. lappa* could be considered as potential herbal drug candidates, which arrest cancer cell proliferation by induction of apoptosis, autophagic, and ferroptosis.

Keywords: apoptosis; asteraceae; autophagy; cell death; lamiaceae; ferroptosis; multiple myeloma; phytotherapy

1. Introduction

Hematologic malignancies are sorts of cancer that originate in the blood-forming tissue such as the bone marrow or the lymph system, and include leukemia, lymphoma, and multiple myeloma (MM) [1]. MM is one of the most common types of hematological cancer and globally accounts for about 10% of all hematologic malignancies. MM is characterized by the accumulation of atypical plasma cells in the bone marrow associated with abnormal production of monoclonal immunoglobulins, which triggers renal complications, hypercalcemia, severe bone pain and destruction, and anemia. The disease is more prevalent among males than females and more in elderly persons [2]. Leukemia is another

life-threatening hematological malignancy, characterized by abnormal elevation number of leucocytes in the blood and bone marrow, resulting from a combination of environmental and genetic factors [3]. Leukemia occurs in adults over the age of 55 years but is the most predominant cancer in children younger than 15 years of age. Among the most common types of leukemia are acute lymphoblastic leukemia and acute myeloid leukemia with a five-year survival rate of 68.2 and 26.9%, respectively [4]. Medicinal plants have drawn great attention as a source for novel oncological therapeutics due to their bioactive chemical ingredients with potential effectiveness and minimal toxicity profiles [5].

Thymus vulgaris is a perennial pleasant-smelling plant of the mint family Lamiaceae and commonly known as thyme. The Kurdish name of the plant is Jatre. The plant grows in coarse, rough soils and sunny climates. It is native to Asia, Europe, America, and Africa [6], and since ancient times has been used as a condiment, perfume, and incense [7]. The plant is known for its essential oil content such as (thymol, carvacrol, β -myrcene, γ -terpinene, linalool, terpinene-4-ol, p-cymene), flavonoids (apigenin, thymonin, luteolin-7-*O*-glucuronide, luteolin-7-*O*-rutinoside, eriodictiol-7-*O*-rutinoside, nobiletin, cirsilineol, and 8-methoxycirsilineol), quinones (arbutin), and phenolic acid (caffeic acid and rosmarinic acid) [8]. Thyme possesses various biological activities including anti-viral, anti-inflammatory, anti-oxidant, anti-cancer, insecticidal, antidiabetic, and anti-spasmodic activities [9]. *T. vulgaris* possess a hepatoprotective effect against acetaminophen-induced hepatic necrosis in mice [10]. According to numerous studies, *T. vulgaris* inhibited the viability of various tumor cell lines in a concentration-dependent manner such as breast cancer, oral cavity squamous cell carcinoma, leukemia, prostate carcinoma, cervical epithelial carcinoma, and lung carcinoma [11,12]. The human colorectal HCT116 cancer cell model was shown to prevent the rate of cell proliferation and stimulated apoptosis associated with increased caspase-3/7 activity [13].

Arctium lappa is a biennial edible flowering plant of the family Asteraceae and commonly known as burdock. The Kurdish name of the plant is Bnawatom. It is found in woods and forests, but mainly alongside roads, waste places, and rivers. It is cultivated in the Hawraman region, southern Kurdistan, Iraq as a medicinal plant [14]. *A. lappa* is native to Europe and Asia and rapidly spread across North America by the early European settlers [15]. The roots of *A. lappa* contain diverse bioactive secondary metabolites such as lignans (arctigenin, arctiin, and diarctigenin), polyphenols (caffeic acid, caffeic acid 4-*o*-glucoside, chlorogenic acid, quercitrin, quercetin, quercetin-3-*O*-glucuronide, nobiletin, p-coumaric acid, biachanin A, and tangeretin), tannin, and terpenoids (lupeol, ursolic, and oleanolic acids) [16]. These ingredients are known for their free-radical scavenging activity, anti-cancer, anti-metastatic, anti-allergic, anti-inflammatory, anti-hepatotoxic and anti-viral potency [17]. Tian, X. et al., reported the neuroprotective effects of the ethyl acetate extract of *A. lappa* roots against H₂O₂ induced cell damage in human neuroblastoma SH-SY5Y cells [18]. Investigation of the effects of *A. lappa* on human cancer cells showed that on the treatment of cells with different extracts, dichloromethane extracts revealed activity, especially for leukemia K562, breast MCF-7 and renal 786-0 cell lines with tumor growth inhibition at 3.62, 41.1, and 60.32 μ g/mL, respectively [19].

T. vulgaris and *A. lappa* are among the commonly used traditional medicines in Iraq for treatment of diseases related to cancer or that may lead to cancer, such as skin diseases, blood-related diseases, inflammatory diseases, immune disorders, and infectious diseases [14,20]. There is little scientific evidence on the cytotoxic activity of *T. vulgaris* and *A. lappa* towards MM cell lines. Therefore, the goal of the present investigation was to evaluate the cytotoxicity of *T. vulgaris* and *A. lappa* extracts against various MM cell lines, to elucidate the mechanisms of cell death and to identify the bioactive compounds present in the most effective extracts.

2. Results

2.1. Cytotoxicity of *T. vulgaris* and *A. lappa*

Butanol and ethyl acetate extracts revealed the best extraction yields among the four extract types in both plants followed by *n*-hexane and chloroform extracts, (Table 1).

Table 1. The proportion of different solvent extractions of *T. vulgaris* and *A. lappa*.

Plants	Solvents	Yields (w/w %)	Color	Consistency
<i>T. vulgaris</i>	<i>n</i> -Hexane	21.172	Dark green	Greasy, semisolid
	Chloroform	2.663	Dark green	Solid
	Ethyl acetate	28.236	Pale yellow	Solid
	Butanol	41.507	Dark red	Gummy
<i>A. lappa</i>	<i>n</i> -Hexane	1.828	Yellowish green	Greasy, semisolid
	Chloroform	0.454	Reddish brown	Solid
	Ethyl acetate	4.217	Reddish brown	Solid
	Butanol	12.756	Dark red	Gummy

The results of the resazurin assay displayed that all fractions exhibited cytotoxic activity in an inhibitory concentration 50 (IC₅₀) range from 2.13 ± 3.77 µg/mL (chloroform fraction (CF) in CCRF-CEM cells) to 94.35 ± 4.60 µg/mL (butanol fraction (BF) in CEM/ADR5000 cells). Among the fractions tested, chloroform and ethyl acetate revealed the highest cytotoxic activity against both cell lines (Table 2). Multidrug-resistant CEM/ADR5000 cells revealed only low degrees of cross-resistance to ethyl acetate fraction (EF), CF and BF of *T. vulgaris* and *n*-hexane fraction (HF), CF and BF of *A. lappa* (range of resistance degrees from 1.88 to 5.71) and were not cross-resistant to HF of *T. vulgaris* and EF of *A. lappa* (degrees of resistance: 1.08 and 1.18). For comparison, CEM/ADR5000 cells exhibit high level cross-resistance to its selection agent, doxorubicin, of more than 1000 and high-level cross-resistant to other natural product-derived anticancer drugs (other anthracyclines, Vinca alkaloids, taxanes, and epidodophyllotoxins) [21].

Table 2. Cytotoxicity of different *T. vulgaris* and *A. lappa* fractions towards leukemia cell lines as determined by resazurin assay.

Fractions	<i>T. vulgaris</i>			<i>A. lappa</i>		
	CCRF-CEM	CEM/ADR5000	D.R.	CCRF-CEM	CEM/ADR5000	D.R.
	IC ₅₀ (µg/mL ± SD)	IC ₅₀ (µg/mL ± SD)		IC ₅₀ (µg/mL ± SD)	IC ₅₀ (µg/mL ± SD)	
HF	31.51 ± 1.63	34.02 ± 0.84	1.08	29.72 ± 1.10	55.93 ± 0.68	1.88
CF	2.13 ± 3.77	4.00 ± 0.15	1.88	6.75 ± 0.95	14.95 ± 3.28	2.21
EF	4.35 ± 1.18	24.85 ± 2.60	5.71	25.38 ± 3.29	29.80 ± 2.32	1.17
BF	28.64 ± 0.35	94.35 ± 4.60	3.29	30.67 ± 2.09	93.48 ± 4.89	3.05

D.R., degree of resistance; HF, *n*-hexane fraction; CF, chloroform fraction; EF, ethyl acetate fraction; BF, butanol fraction. Values are presented as the mean ± SD.

Both fractions were further investigated against 9 MM cell lines (Table 3). *Thymus* chloroform fraction (TCF) and *Arctium* chloroform fraction (ACF) demonstrated greatest growth inhibitory activity compared to *Thymus* ethyl acetate fraction (TEF) and *Arctium* ethyl acetate fraction (AEF) against all examined MM cancer cell lines, especially NCI-H929 cells for TCF (IC₅₀: 6.49 ± 1.48 µg/mL) and RPMI-8226 for ACF (IC₅₀: 18.26 ± 0.26 µg/mL).

Compared to leukemia and MM cell lines, these extracts did not display cytotoxicity against non-cancerous peripheral blood mononuclear cells (PBMCs) up to 100 µg/mL (Figure 1A). TEF showed the lowest activity in MOLP-8 (IC₅₀: 41.63 ± 0.53 µg/mL) and AEF demonstrated no obvious cytotoxic effect of up to 100 µg/mL in RPMI-8226 cells after 72 h incubation.

The data in Figure 1b demonstrate the influence of ferroptosis inhibitors. Both ferrostatin-1 and deferoxamine nullified the cytotoxic activity of TCF and ACF up to the highest concentration tested (100 µg/mL).

Table 3. Cytotoxicity of chloroform and ethyl acetate fractions of *T. vulgaris* and *A. lappa* towards MM cell lines as determined by the resazurin assay.

MM Cell Line	<i>T. vulgaris</i>		<i>A. lappa</i>	
	IC ₅₀ (µg/mL ± SD)		IC ₅₀ (µg/mL ± SD)	
	CF	EF	CF	EF
MOLP-8	13.45 ± 3.49	41.63 ± 0.53	39.51 ± 2.30	56.92 ± 1.00
NCI-H929	6.49 ± 1.48	25.55 ± 3.78	21.9 ± 0.69	35.01 ± 0.94
RPMI-8226	27.14 ± 0.01	30.17 ± 0.17	18.26 ± 0.26	>100
KMS-12BM	15.28 ± 4.90	31.78 ± 3.46	22.3 ± 0.18	81.2 ± 1.78
KMS-11	17.26 ± 2.48	35.15 ± 1.93	31.95 ± 2.37	65.04 ± 1.89
L-363	11.28 ± 4.64	25.61 ± 2.21	46.97 ± 3.66	35.62 ± 0.43
JJN-3	13.88 ± 1.19	30.11 ± 1.69	25.99 ± 0.70	48.00 ± 4.41
AMO-I	14.02 ± 2.64	35.07 ± 3.23	29.11 ± 1.04	35.02 ± 0.59
OPM-2	6.91 ± 3.70	26.06 ± 0.78	35.63 ± 4.079	45.96 ± 2.49

MM, multiple myeloma; CF, chloroform fraction; EF, ethyl acetate fraction. Values are presented as the mean ± SD.

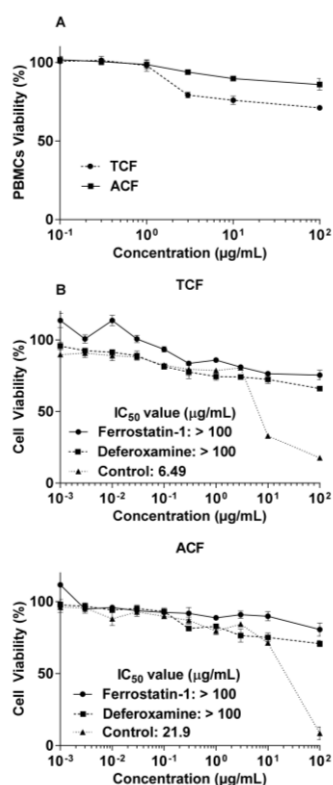


Figure 1. Cytotoxicity of chloroform fractions of *T. vulgaris* (TCF) and *A. lappa* (ACF) towards NCI-H929 cells and peripheral blood mononuclear cells (PBMCs) as determined by the resazurin assay. (A): Cytotoxicity towards normal PBMCs. (B): The ferroptosis inhibitors (ferrostatin-1 and deferoxamine) abrogated cytotoxicity of the extracts, indicating the role of ferroptosis cell death. Control: NCI-H929 cell without ferroptosis inhibitors.

2.2. Apoptosis via Intracellular ROS Generation and MMP Disruption

Annexin V-FITC/PI staining was used to determine whether apoptosis as a mode of cell death is involved in TCF- and ACF-promoted growth inhibition in NCI-H929 cells. As shown in Figure 2, the treatment of NCI-H929 cells with TCF induced late apoptosis (66% and 71% vs. 6% and 5% for untreated cells). On the other hand, exposure to ACF also induced late apoptosis (40% and 50% vs. 6% and 5% for untreated cells) and late necrosis (13% and 17% vs. 4% and 6% for untreated cells). For visualization of morphologic features of apoptotic cell death,

we performed 4',6-diamidino-2-phenylindole (DAPI) staining following inoculation of NCI-H929 cells with 1 and 2 \times IC₅₀ of TCF and ACF for 48 h. Figure 2 showed clear apoptotic features such as apoptotic bodies formation, chromatin condensation, nuclear fragmentation, as well as cell shrinkage.

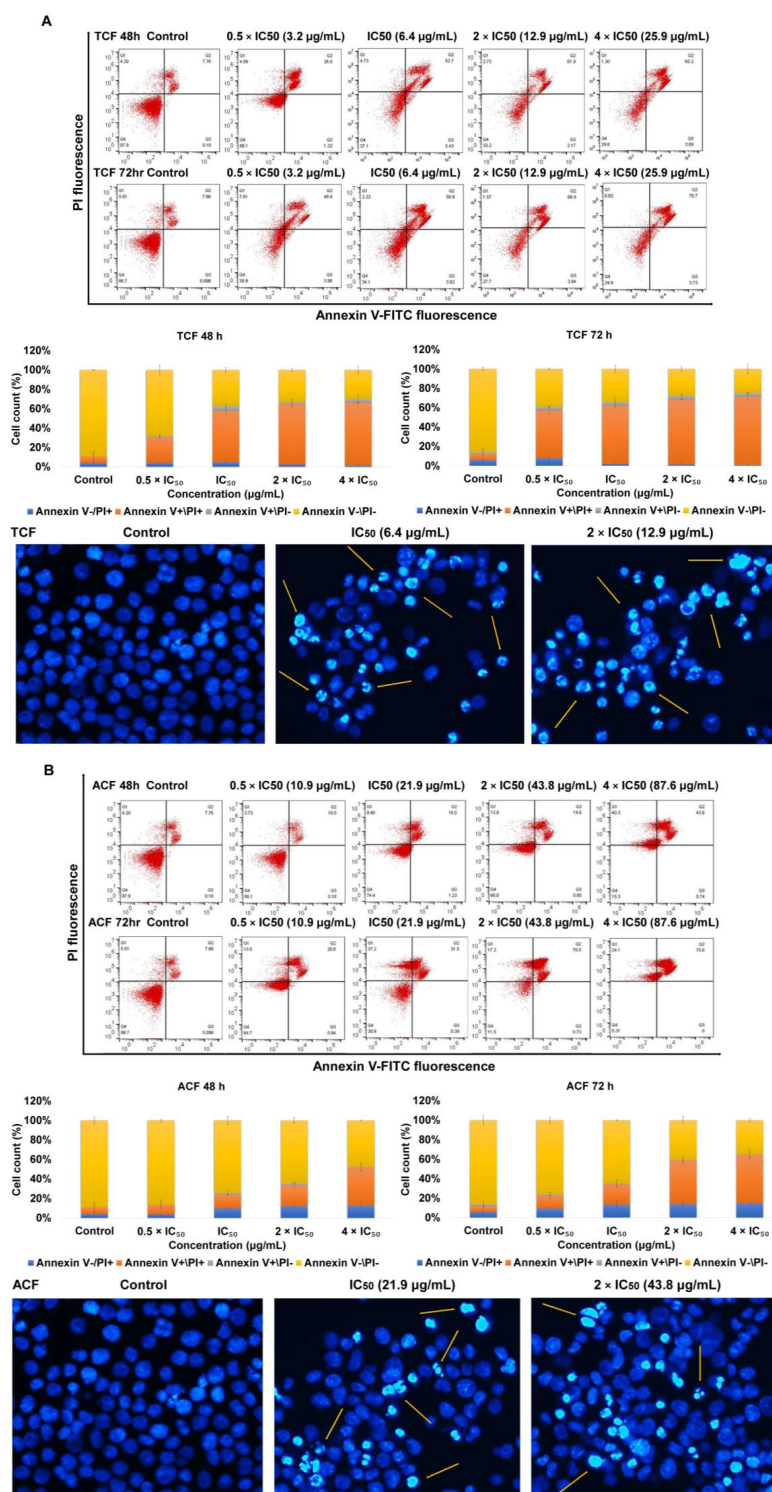


Figure 2. Apoptosis induction in NCI-H929 cell lines. Annexin V/PI assay of NCI-H929 cells incubated with 0.5, 1, 2, 4 \times IC₅₀ of chloroform fractions of (A)-*T. vulgaris* (TCF) and (B)-*A. lappa* (ACF) for 48 and 72 h. Morphology of NCI-H929 cell was noticed under fluorescence microscope by using 4',6-diamidino-2-phenylindole (DAPI) stain. Yellow arrows referred to apoptotic features were observed in A-TCF and B-ACF treated cells vs. untreated cells. Control: NCI-H929 cell without treatment.

To find out whether TCF- and ACF-induced apoptosis was correlated with reactive oxygen species (ROS) generation and breakdown of mitochondrial membrane potential (MMP), we assessed ROS level and MMP integrity. After exposure of NCI-H929 cells to 0.5, 1, 2, 4 \times IC₅₀ concentrations of TCF and ACF stained with 2',7'-dichlorodihydrofluorescein diacetate (H2DCFH-DA), we observed obvious elevations of ROS levels in treated cells compared to untreated cells. As presented in Figure 3, ROS generation was elevated by 7.8-, 9.5-, and 4.6-fold following 1 h treatment with TCF, ACF, or hydrogen peroxide H₂O₂ (as positive control), respectively.

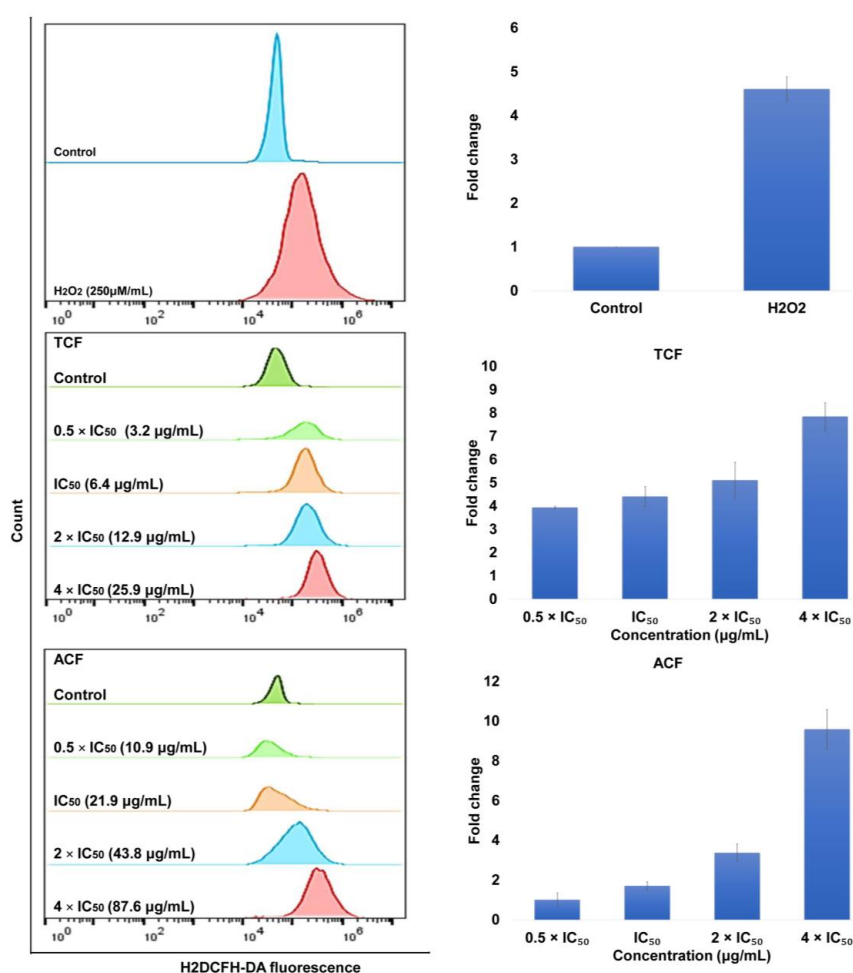


Figure 3. Intracellular production of reactive oxygen species in NCI-H929 cells. Results following 1 h incubation with 0.5, 1, 2, 4 \times IC₅₀ of chloroform fractions of *T. vulgaris* (TCF) and *A. lappa* (ACF), stained with 2',7'-dichlorodihydrofluorescein diacetate (H2DCFH-DA) and analyzed by flow cytometry. Control: NCI-H929 cell without treatment.

The loss of MMP is indicated by a decrease in the ratio of red/green fluorescence intensity. Figure 4 shows the addition of TCF and ACF at 0.5, 1, 2, 4 \times IC₅₀, as well as valinomycin (positive control), for 24 h reduced the ratio of red (JC-1 aggregates) fluorescence to green (JC-1 monomers) fluorescence in a dose-dependent manner and the minimum ratio revealed on exposure to TCF (4 \times IC₅₀: 0.19%), followed by valinomycin (20 μ M: 0.2%) and ACF (4 \times IC₅₀: 0.61%) in comparison to untreated NCI-H929 cells (70.42%). These findings indicate that apoptosis promoted by *T. vulgaris* and *A. lappa* was associated with ROS generation and disruption of MMP integrity.

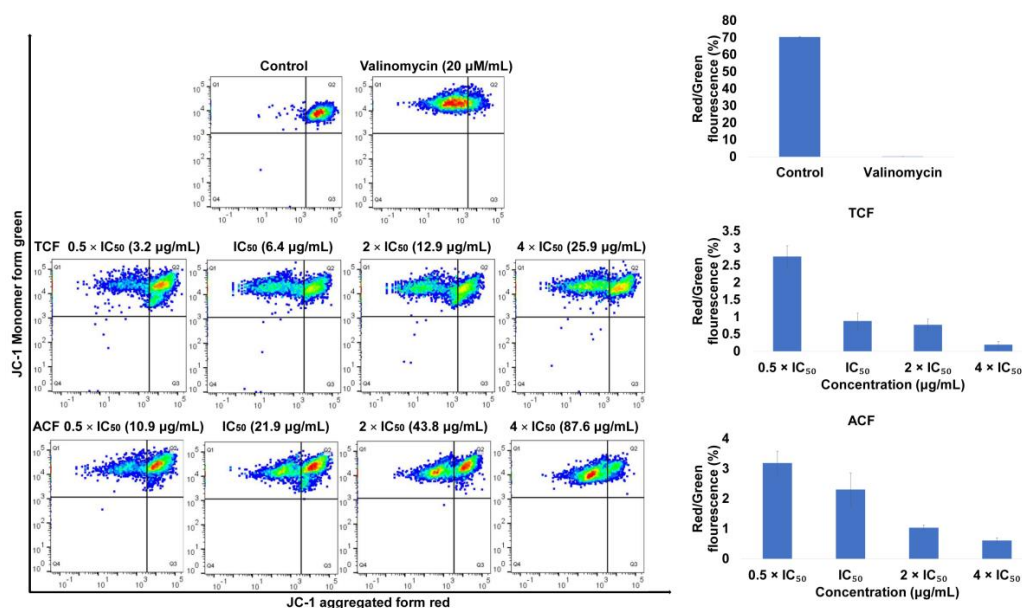


Figure 4. Disruption of mitochondrial membrane potential (MMP) in NCI-H929 cells exposed to 0.5, 1, 2, 4 \times IC_{50} of chloroform fractions of *T. vulgaris* (TCF) and *A. lappa* (ACF) for 24 h, stained with 5,5',6,6'-tetrachloro-1,1',3,3'-tetraethylbenzimidazolyl carbocyanine iodide (JC-1) and analyzed by flow cytometry. The ratio of red (JC-1 aggregate)/green (JC-1 monomer) fluorescence was used to display the effect of TCF, ACF, and valinomycin on the MMP integrity. Control: NCI-H929 cell without treatment.

2.3. Effect of TCF and ACF on Cell Cycle Distribution

NCI-H929 cells were treated with various concentrations of TCF and ACF for 24, 48, and 72 h, stained with propidium iodide (PI) and analyzed using flow cytometry. The results in Figure 5 for TCF show that the cells accumulated in the (apoptotic) sub-G0/G1-phase (14.4%, 16% and 48.4%, vs. 10%, 12%, and 9.25% for untreated cells) following 24, 48, and 72 h, respectively. Furthermore, the cells arrested in the G2/M-phase (20% and 26%, vs. 18% and 20% for untreated cells) after 24 and 48 h, respectively, with corresponding decreases in proportion of cells arrested in the G0/G1-phase (57.5%, 42%, and 24.4% vs. 60.7%, 55%, and 59% for untreated cells). Additionally, the exposure of NCI-H929 cells to ACF resulted in arresting of cells in the sub-G0/G1-phase (13%, 26%, and 42.8%, vs. 10%, 12%, and 13% for untreated cells) following incubation for 24, 48, and 72 h, respectively, and G2/M-phase (25.1% and 19%, vs. 20% and 17% for untreated cells) after 48 and 72 h, respectively, with corresponding decreases in the ratio of cells in the G0/G1-phase (59%, 33%, and 28.7% vs. 60.7%, 55%, and 58% for untreated cells).

2.4. TCF and ACF Affects the Expression of Beclin-1 and LC3B-II

Following the treatment of NCI-H929 cells with TCF or ACF (1, 2, or 4 \times IC_{50}) for 24 h, the results in Figure 6 showed an elevated expression of Beclin-1 and LC3B-II compared to untreated control.

2.5. Phytochemical Study of TCF and ACF

Liquid chromatography-electrospray ionization-mass spectrometer (LC-ESI/MS) analysis for TCF and ACF demonstrated the presence of 5–20 constituents in chloroform fractions of each plant. In Figure 7, the chromatogram of TCF revealed that the peaks no. 1 and 2 were predicted to be apigenin and nobiletin, while in the chromatogram of ACF peaks no. 2, 3, and 4 were predictive to be nobiletin, ursolic acid, and lupeol. These compounds were identified by comparison of our m/z values, MS/MS spectra, and the chemical formula by concomitant injection with authentic standard compounds and compared their retention time values.

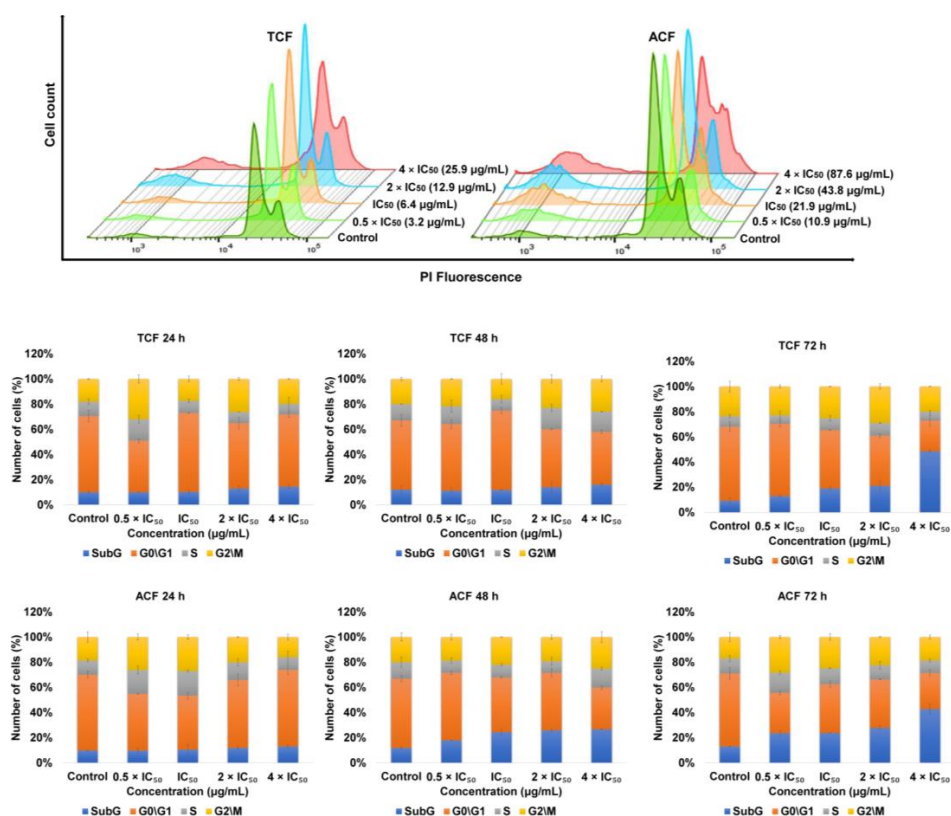


Figure 5. Induction of cell cycle disturbance in NCI-H929 cell lines treated with 0.5, 1, 2, 4 × IC₅₀ of chloroform fractions of *T. vulgaris* (TCF) and *A. lappa* (ACF) following 24, 48, and 72 h, stained with propidium iodide (PI) and analyzed by flowcytometry. Control: NCI-H929 cell without treatment.

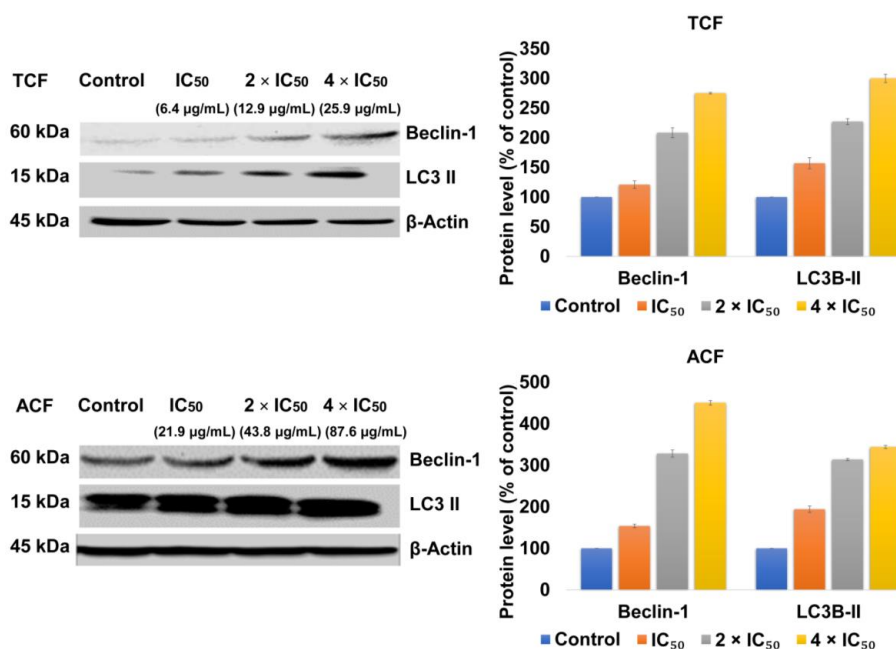


Figure 6. The expression of Beclin-1 and LC3B-II in human NCI-H929 cells treated with 1, 2, 4 × IC₅₀ of chloroform fractions of *T. vulgaris* (TCF) and *A. lappa* (ACF) for 24 h was detected by western blot analyses. The relative protein expression of Beclin-1 and LC3B-II was normalized to β-actin. Control: NCI-H929 cell without treatment.

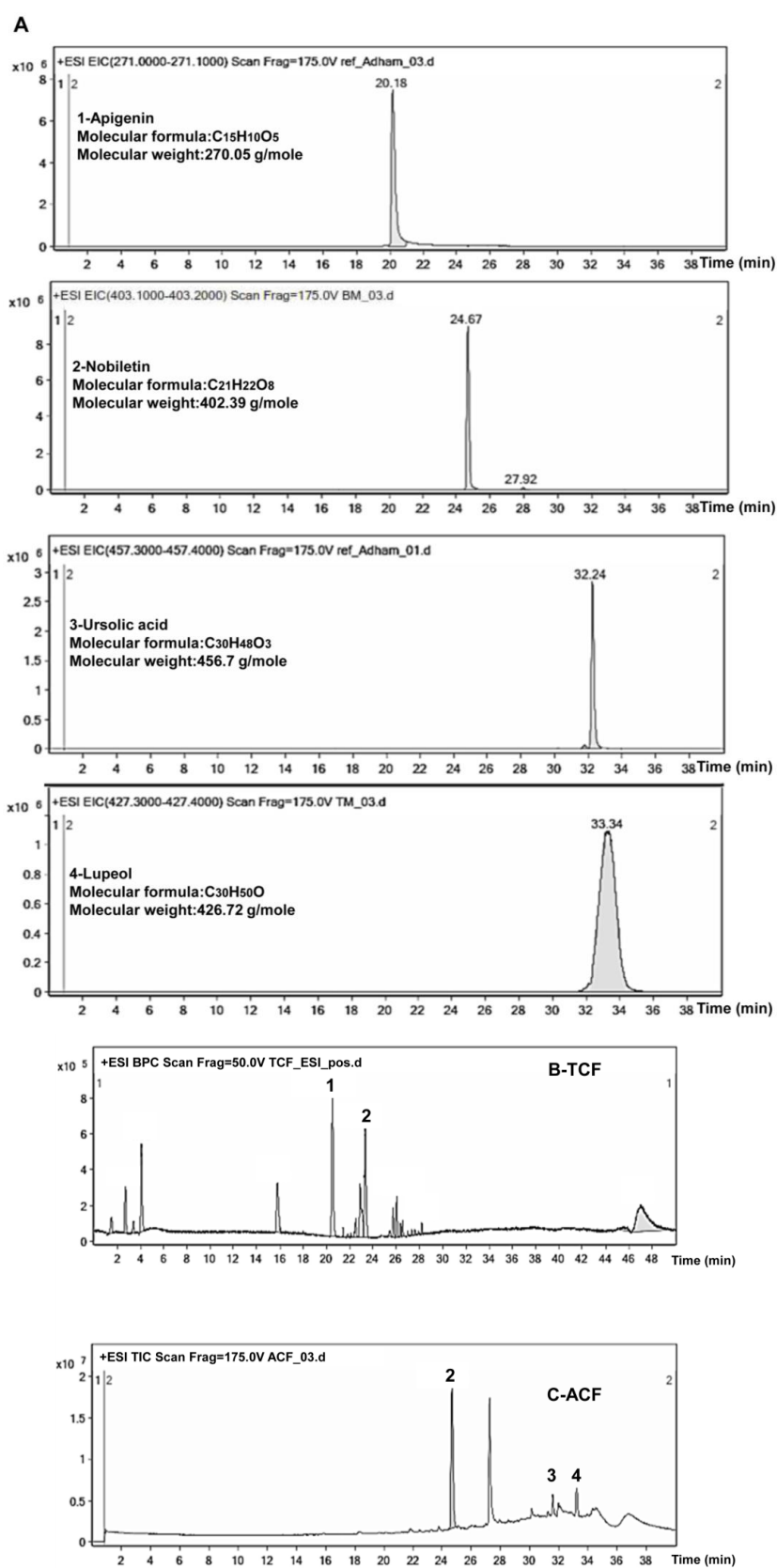


Figure 7. LC-ESI/MS chromatograms *T. vulgaris* and *A. lappa* extracts. **(A)**-Standard compounds. (1) Apigenin, (2) Nobiletin, (3) Ursolic acid, and (4) Lupeol. **(B)**-*T. vulgaris* chloroform fraction (TCF) and **(C)**-*A. lappa* chloroform fraction (ACF).

3. Discussion

The cytotoxic activity of *T. vulgaris* and *A. lappa* towards various cancer cell lines was previously reported [11,12,19]. Several reports provided evidence on the activity against cell lines derived from solid tumors but very few data were available about their activity on MM cell lines. In our study, four fractions of *T. vulgaris* and *A. lappa* with different polarities were screened using the resazurin reduction assay against drug-sensitive CCRF-CEM and multidrug-resistant P-glycoprotein-overexpressing CEM/ADR5000 cells. All fractions showed cytotoxic activity against both cell lines with IC₅₀ value between 2.13 ± 3.77 to 94.35 ± 4.60 µM/mL. Doxorubicin exhibited cytotoxic activity against sensitive and resistant phenotypes of leukemia cells such as CCRF-CEM cells and CEM/ADR5000 with IC₅₀: 0.02 ± 0.00 and 122.96 ± 10.94 µM/mL [22]. CEM/ADR5000 were more sensitive to *T. vulgaris* and *A. lappa* extracts than Doxorubicin. According to the American National Cancer Institute, plant extracts with IC₅₀ values < 30 µg/mL following 72 h incubation can be considered as reasonable strong cytotoxic activity [23]. Chloroform and ethyl acetate fractions of both plants met the required criteria for IC₅₀ values in the range between 2.13 and 29.80 µg/mL for CCRF-CEM and CEM/ADR5000 cells. Thus, leukemia cell lines were highly sensitive to semi-polar compounds present in chloroform and ethyl acetate fractions as compared to polar and nonpolar compounds [24]. In another report, extracts of *T. vulgaris* revealed a dose-dependent reduction of THP-1 leukemia cell viability with an IC₅₀ value of 156.9 µg/mL, while the toxicity towards normal human PBMCs was much less (IC₅₀: 334.5 µg/mL) [11]. In our analyses, TCF and TEF revealed the highest cytotoxicity towards NCI-H929 cells with IC₅₀ values of 6.49 ± 1.48 µg/mL and 25.55 ± 3.78 µg/mL, respectively. Doxorubicin prevents human MM cell lines such as RPMI 8226, U266, and NCI-H929 via apoptosis induction [25]. Cell death typically occurs by apoptosis, necrosis, ferroptosis, autophagy, pyroptosis, mitotic catastrophe, and so on. Apoptosis, also known as programmed cell death, a characteristic form of cell death, is controlled, energy-dependent and no inflammation is accompanying it [26]. TCF suppressed cell growth, induced apoptosis (late apoptosis) mainly accompanied by disruption of MMP integrity, affected cell cycle phase especially sub-G₀/G₁ in dose-time dependent manner in NCI-H929 cell lines, and slightly affected the G₂/M phase at various concentrations. These results are in line with previous reports suggesting that polyphenolic extracts from *T. vulgaris* inhibited cell viability and promoted apoptosis in neuroblastoma cells, e.g., SH-SY5Y and SK-N-BE(2)-C cell lines at doses of 62.5 and 125 µg/mL [27]. Furthermore, the ethanolic extract arrested the cell cycle at the G₂/M phase of T-47D breast cancer cells [28]. On the other hand, ACF displayed the greatest cytotoxicity against RPMI-8226 cells (IC₅₀: 18.26 ± 0.26 µg/mL) and AEF against NCI-H929 cells (IC₅₀: 35.01 ± 0.94 µg/mL). ACF inhibited cell growth, promoted necrosis and apoptosis (late apoptosis) that was mainly associated with ROS generation and induction of cell cycle arrest at a sub-G₀/G₁ phase in NCI-H929 cell lines, and at the same time slightly affected G₂/M phase. However, previous studies reported that an ethanol extract of *A. lappa* root exhibited profound cytotoxic potency against Jurkat T-cell leukemia cells upon treatment for 24 h (IC₅₀: 102.2 ± 42.4 µg/mL), by DNA fragmentation and induction of intrinsic apoptosis associated with loss of MMP and activation of caspase-3/7 without toxicity towards non-cancerous murine embryonic 3T3 fibroblasts [29]. *A. lappa* induced G₀/G₁ cell cycle arrest in gastric cancer cell lines as well as disturbance of the G₂/M phase in colon cancer cells [30]. Our study showed that ferroptosis cell death in addition to apoptosis was involved in the tumor-suppressive activities of TCF and ACF. To the best of our knowledge, this is the first report regarding ferroptosis for these two plants. Ferroptosis is a novel form of cell death that is programmed necrosis and for the first time proposed in 2012 by Dixon [31,32]. It plays an essential role in the cessation of tumorigenesis by eliminating the cells that are scratched by infection or lacking in the main nutrients in the environment. Several studies have shown that the chief causative factor in triggering ferroptosis is the classic oxidative stress pathway. Erastin was the first introduced ferroptosis-inducing agent, followed by cisplatin, temozolomide, artesunate, sulfasalazine [33]. Interestingly, culturing NCI-H929 cells treated with TCF or ACF showed an upregulation of important autophagy-related markers such as LC3B-II and Beclin-1, implying the ability of both plants to induce autophagy. Beclin1 the

mammalian orthologue of yeast Atg6, contributes as a scaffold, in the initial step for the autophagy process, which is the construction of phosphatidylinositol 3 kinases (PI3K) complex and present on the human chromosome 17q21. Beclin1 overexpression suppressed proliferation, and reduced the cell viability, by triggering autophagic cell death via the evolutionarily conserved domain and the coiled-coil domain bind to Vps34p and UVRAG, respectively [34]. LC3B-II belongs to the microtubule-associated protein 1A/1B-light chain 3 (LC3) family and accumulates particularly on nascent autophagosomes. Cytosolic-associated protein light chain 3 (LC3-I) converted to the membrane-bound LC3-II form on autophagosome formation [35]. ACF possessed higher efficacy compared to TCF. Apigenin and nobiletin were identified in the TCF, while nobiletin, lupeol, and ursolic acid were detected in ACF. The available literature demonstrated that flavonoids and terpenoids are abundant in vegetables, fruits, and medicinal herbs and revealed cytotoxicity towards several human cancer cell lines and induced cell death through various mechanisms [36]. A recent study reported that in MM cells, apigenin treatment potentially inhibited cell development in a concentration-dependent manner by inducing cell apoptosis, ferroptosis, and autophagy, associated with down-regulating of STAT1, and Akt with concomitant activation of caspases, JNK, P-38 MAPK, Beclin-1, and LC3 II [37]. In human papillary thyroid carcinoma BCPAP cells, apigenin induced G2/M cell cycle arrest and DNA damage through suppressing the expression of Cdc25c and triggering the accumulation of ROS production [38]. Nobiletin repressed the development of human gastric TMK-1 cell lines, (IC_{50} : 134.8 μ M) through induction of apoptosis and cell cycle arrest in the G0/G1 phase [39], and suppress the expression of the crucial factor for endoplasmic reticulum stress such as thioredoxin-interacting protein (TXNIP), and consequently leads to cell apoptosis in human neuroblastoma cells [40]. Ursolic acid promoted apoptotic cell death in human breast cancer MCF-7 cells by Bcl-2 downregulation and suppressing the expression of transcription factor FoxM1 [41], while in MDA-MB-231 cells via mitochondrial death and extrinsic death receptor pathway [42]. Another study stated that ursolic acid triggered autophagy cell death in glioma U87MG cells through the formation of acidic vesicular organelles, the development of autophagolysosomes, and the accumulation of LC3-II [43]. Lupeol has shown cytotoxic activity toward MM RPMI 8226 (IC_{50} : 50 μ M), lung carcinoma A-549 (IC_{50} : 50 μ M), breast carcinoma MCF-7 (IC_{50} : 50 μ M), malignant melanoma G361 (IC_{50} : 50 μ M), and cervical carcinoma HeLa (IC_{50} : 37 μ M), following 72 h incubation [44]. Apoptosis induction of lupeol in human promyelotic leukemia HL-60 cells exhibited through the creation of hypodiploid nuclei and fragmentation of DNA in a concentration and time-dependent way [45].

4. Material and Methods

4.1. Chemicals and Reagents

Solvents such as *n*-hexane, chloroform, ethyl acetate, butanol, acetonitrile, and methanol were purchased from Chem-Lab (Zedelgem, Belgium). Penicillin and streptomycin were obtained from Gibco (Co Dublin, Ireland). Annexin V-FITC/PI detection apoptosis kit was obtained from Life Technologies (Carlsbad, CA, USA) and 5,5',6,6'-tetrachloro-1,1',3,3'-tetraethylbenzimidazolyl carbocyanine iodide (JC-1) kits from Biomol (Hamburg, Germany). H2DCFH-DA, H₂O₂, ferrostatin-1, deferoxamine, valinomycin, PI, resazurin, triton X-100, paraformaldehyde, tween-20, dimethylsulphoxide (DMSO), DAPI and doxorubicin (98.0% purity) were purchased from Sigma-Aldrich (Taufkirchen, Germany). M-PER[®] mammalian protein extraction reagent and protease inhibitor were obtained from Thermo Fisher Scientific (Waltham, MA, USA). Antibodies against Beclin-1 (D40C5), LC3B, β -actin (D6A8) and anti-rabbit IgG HRP-linked antibody were purchased from Cell Signaling Technology (Danvers, MA, USA) and Luminata[™] Classico Western HP substrate was obtained from Merck Millipore (Darmstadt, Germany).

4.2. Preparation of Plant Extracts

Aerial parts of *T. vulgaris* and roots of *A. lappa* were collected from the Kurdistan region, Iraq, during 2018–2019. The plant materials were authenticated by assistant professor Al-Khayat AH, and vouchers (A-11 and A-12, respectively) were deposited at Pharmacognosy Department, Pharmacy College, Hawler Medical University. Powdered plant materials (each 500 g) were extracted successively in a Soxhlet extractor [46] with methanol for 36 h. The extracts were concentrated to dryness by using a rotary vapor machine at 40–50 °C (Buchi Rotavator®, Switzerland) and re-dissolved in 10% methanol, followed by liquid-liquid fractionation using (10×) with an equal volume of *n*-hexane, chloroform, ethyl acetate, and butanol solvents. The obtained fractions of HF, CF, EF, and BF were concentrated under vacuum and subsequently powdered using a freeze-dryer (Martin Christ Alpha 1–2 LD plus, Osterode am Harz, Germany) to provide fractions with diverse polarity. All fractions were kept at 4 °C for further investigations.

4.3. Cell Culture Conditions

Nine multiple myeloma cell lines, MOLP-8, NCI-H929, RPMI-8226, KMS-12BM, KMS-11, L-363, JJN-3, AMO-I, and OPM-2 were kindly provided by Ellen Leich-Zbat (Institute of Pathology, University of Würzburg, Germany) [47]. Sensitive CCRF-CEM and multidrug-resistant CEM/ADR5000 leukemia cells were obtained from Prof. Axel Sauerbrey (Department of Pediatrics, University of Jena, Germany). The multidrug resistance phenotype of CEM/ADR5000 cells has been previously characterized [21,48]. The cell lines were cultured in Roswell Park Memorial Institute (RPMI 1640) medium (Gibco, Co Dublin, Ireland), supplemented with 10% fetal bovine serum (FBS) (Gibco, Co Dublin, Ireland), and 1% penicillin (100 U/mL)-streptomycin (100 µg/mL) in a humidified atmosphere with 5% CO₂ at 37 °C. The resistance of CEM/ADR5000 cell lines has been maintained by adding 5000 ng/mL doxorubicin. PBMCs were isolated and cultivated as reported previously [49].

4.4. Resazurin Reduction Assay

The cell viability of cells was studied by means of the cell-permeable redox indicator resazurin. Briefly, 1×10^4 cells/well of MM and leukemia cells were suspended in 100 µL of the growth medium, plated in 96 well plates; then the volume was increased to 200 µL/well by treating the cells with 100 µL of medium containing various concentrations of plant extract (0.001–100 µg/mL), previously dissolved in DMSO (final concentration 0.3%). Cells treated with 0.3% DMSO were considered as a negative control [50]. The resazurin assay was also used to investigate the influence of ferroptosis inhibitors such as ferrostatin-1 and iron chelators deferoxamine on the cytotoxicity of various plant fractions as previously described [51]. Further, 1×10^4 NCI-H929 cells/well were cultured with ferrostatin-1 (50 µM) and deferoxamine (0.2 µM) for 1 h before exposure to treatment. Subsequently, cells incubated with different concentrations of plant fractions (0.001–100 µg/mL) and control. After 72 h incubation in a 5% CO₂ environment at 37 °C, 20 µL 0.01% *w/v* resazurin solution was added to each well and incubated in the dark for a further 4 h. The resazurin fluorescence was measured at an excitation wavelength 544 nm and emission at 590 nm using an Infinite M2000 Pro™ plate reader (Tecan, Crailsheim, Germany). The IC₅₀ of different cell lines was calculated from a calibration curve by exponential linear regression using GraphPad Prism6 software and expressed in mean ± SD. The degree of resistance was determined as the IC₅₀ value of the resistant cell line over the IC₅₀ value of the sensitive cell line [22]. The experiments were repeated three times.

4.5. Flow Cytometric Assessment of Apoptosis

NCI-H929 cells (10^6 cells/well) were treated for 48 or 72 h with various concentrations of TCF and ACE, then incubated at 37 °C and 5% CO₂ atmosphere. Cells were harvested and resuspended in Annexin V-binding buffer. Subsequently, 5 µL Annexin V-FITC and 10 µL PI were added and incubated for 15–20 min in the dark place and room temperature [52]. Cell apoptosis and necrosis were

determined using BD Accuri™ C6 flow cytometer (BD Biosciences, Heidelberg, Germany). The results evaluated using FlowJo software version 7.0. and each experiment was conducted three times. The data expressed as the percentage of cells in each population (viable cell annexin V−/PI−; early apoptotic annexin V+/PI−; late apoptotic annexin and early necrotic V+/PI+; late necrotic V−/PI+).

4.6. Flow Cytometric Assessment of Mitochondrial Membrane Potential

Briefly, 24 h after plating the NCI-H929 cells (10^6 cells/well) with various concentrations of TCF and ACF, 0.3% DMSO (negative control) and valinomycin (positive control), at 37 °C and 5% CO₂ incubation, cells were then incubated with JC-1 for 30 min. The cells were analyzed using the LSR-Fortessa FACS analyzer (Becton-Dickinson, Heidelberg, Germany) and ratio of red/green fluorescence intensity was used to determine alteration in integrity of the MMP and calculated using FlowJo software version 7.0 [53,54]. Each observation was conducted three times.

4.7. Flow Cytometric Assessment Reactive Oxygen Species

NCI-H929 cells (2×10^6 cells/well) were resuspended in phosphate buffer saline (PBS) (Gibco, Co Dublin, Ireland) and exposed to 2 μM of H₂DCFH-DA for 30 min. Subsequently, the cells were treated with various concentrations of TCF and ACF, H₂O₂ (positive control), or DMSO (negative control). After incubation for 1 h, the treated cells were washed twice to remove the extracellular compound and suspended in PBS. The 2',7'-dichlorofluorescein fluorescence was detected using flow cytometry [55]. The amount of ROS achieved was calculated using FlowJo software version 7.0. Each experiment was conducted three times.

4.8. Flow Cytometric Assessment of Cell Cycle Distribution

NCI-H929 cells (10^6 cells/well) were incubated with various concentrations of TCF and ACF for 24, 48, and 72 h at 37 °C and 5% CO₂. DMSO (0.3%) was used as a negative control. Cells were harvested and fixed by adding 1 mL cold absolute ethanol gradually with vortexing to the cell pellet and stored at −20 °C for 24 h. The cells were harvested and washed with PBS, and the nuclei were stained with PI at a final concentration of 50 μg/mL. The percentage of DNA contents in each phase (sub-G₀/G₁, G₀/G₁, S and G₂/M) was measured using a BD Accuri™ C6 flow cytometer [56]. Each experiment was conducted three times.

4.9. Fluorescence Microscopy

Following 48 h treatment of NCI-H929 cells (10^6 cells/well) with various concentrations of TCF and ACF, the cells were fixed with 4% paraformaldehyde for 30 min at room temperature, washed with PBS, and blocked with 5% FBS and 0.1% Triton X-100 in PBS for a further 1 h at room temperature. The nuclear morphology of apoptotic cells was monitored by staining cell nuclei with 1 μg/mL of DAPI [57], in the dark for 10 min, at 37 °C and visualized under a fluorescent microscope (EVOs FL Cell Image System, Thermo Fisher Scientific).

4.10. Western Blotting

NCI-H929 cells (10^6 cells/well) were treated with various concentrations of TCF and ACF or 0.3% DMSO as a negative control. Following 24 h incubation, the cells were lysed with Mammalian Protein Extraction Reagent M-PER® and protease inhibitor at ratio (1:100) at 4 °C for 30 min. Protein concentrations were determined by Nano-Drop1000 spectrophotometer (Thermo Fisher Scientific). Isolated protein was mixed with sodium dodecyl sulfate-polyacrylamide gel electrophoresis (SDS-PAGE) loading dye and boiled at 95 °C for 10 min. The equal quantity of protein (30 μg) was subjected to 10% SDS-PAGE and subsequently transported to polyvinylidene difluoride membranes (RotiR PVDF, pore size 0.45 μm, Carl Roth GmbH, Karlsruhe, Germany). Further, 5% (*w/v*) bovine serum albumin (Sigma-Aldrich, Darmstadt, Germany) in Tris-buffered saline containing 0.5%

tween-20 (BSA/TBST) was used to block the non-specific binding sites in the membranes at room temperature for 1 h. The membranes were incubated with antibodies against LC3B, Beclin-1 or β -actin (as normalizing control) overnight at 4 °C. After washing with TBST, the membranes were further incubated with HRP-linked secondary anti-rabbit antibody for 1 h at room temperature. The detection of protein band was carried out by exposing the membrane to Luminata™ Classico Western HRP substrate, and images of the membranes were captured with the Alpha Innotech Fluor Chem Q system (Biozym, Germany) [58]. Image Studio Lite Software was used for the determination of relative band intensity.

4.11. LC-ESI/MS Analysis of *T. vulgaris* and *A. lappa* Fractions

TCF and ACF were analyzed by LC-ESI/MS system. The high-performance liquid chromatography (HPLC) system was 1260 Infinity II (Agilent Technologies, Waldbronn, Germany). A reversed-phase Eclipse Plus C₁₈ RRHP (50 × 2.1 mm, 1.8 μ m particle size, from Agilent Technologies) was used for the separation process. The eluents consisted of 2% acetonitrile in H₂O (Phase A) and 100% methanol (Phase B), and the following gradient mode was used: 0–1 min, 15% B isocratic; 1–24 min, linear gradient from 15% to 95% B; 24–29 min, 95% B isocratic; 29–30 min, linear gradient from 95% to 15% B; and re-equilibration 30–50 min, 15% B isocratic. The column temperature was set to 30 °C, the flow rate to 0.2 mL/min, and the injection volume of 5 μ L. HPLC coupled to a 6545 quadrupole time of flight mass spectrometer (Agilent Technologies) equipped with an Agilent Jet Stream electrospray ionization interface working in the positive mode. High-purity nitrogen was used as the nebulizer and auxiliary gas, and conditions were set at drying gas temperature 320 °C, sheath gas temperature 350 °C, and a flow rate of 10 L/min. The nebulizer pressure set to 35 PSIG, capillary voltage 3.5 kV, nozzle voltage 1 kV. The fragment was set to 175 (arbitrary units). Full MS scans from m/z 100–3000 Da were acquired at a scan rate of 1 spectrum/s. Data processing was performed using mestrenova software.

5. Conclusions

Different fractions of *T. vulgaris* and *A. lappa* inhibited proliferation and reduced cell viability of leukemia and MM cell lines rather than normal human PBMCs in a concentration-dependent manner. As a consequence, our study demonstrated that both plants possess potent cytotoxic activity against hematologic malignancies, the results were supported by an evaluation of their mechanism of action. Among various fractions, TCF and ACF as potent cytotoxic fractions induced apoptosis (as shown in the sub-G₀/G₁ fraction) and slightly arrested cell cycle progression in the G₂/M phase. TCF triggered late apoptosis and early necrosis, while ACF triggers late apoptosis and both early and late necrosis mediated by MMP disruption and increased intracellular ROS levels, which was further emphasized by distinctive morphological changes. The autophagic effects of ACF were greater than that of TCF. In addition to the mentioned mechanisms, ferroptosis cell death was also promoted by TCF and ACF in NCI-H929 cells. LC-ESI/MS analysis exhibited a variety of chemical constituents in TCF and ACF, four of which were identified as apigenin, nobiletin, lupeol, and ursolic acids.

Author Contributions: Conceptualization, A.M.N. and T.E.; methodology, A.M.N., T.E. and M.E.F.H.; formal analysis, T.E.; validation, A.M.N. and T.E.; investigation, A.N.A. and M.E.F.H.; resources, A.M.N. and T.E.; writing—original draft preparation, A.N.A.; writing—review and editing, A.M.N., T.E. and M.E.F.H.; visualization, T.E. and A.N.A.; supervision, A.M.N. and T.E.; project administration, A.M.N. and T.E.; funding acquisition, A.M.N. and T.E. All authors have read and agreed to the published version of the manuscript.

Funding: A.N.A. is grateful for a stipend of the Hawler Medical University to visit the Department of T.E. The consumables were equally financed by the Hawler Medical University, the Johannes Gutenberg University, and a donation of Marc Strobel, Frankfurt. M.E.F.H. acknowledges the financial support from Alexander von Humboldt Foundation, Germany “Georg Forster Research Fellowship for Experienced Researchers”.

Acknowledgments: Authors are grateful to the Institute of Molecular Biology gGmbH (IMB) (Mainz, Germany), where the flow cytometry experiments for MMP were performed. The authors also gratefully acknowledge the Core Facility for Mass Spectrometry at the Department of Chemistry of Johannes Gutenberg University in Mainz for performing LC-ESI/MS analysis.

Conflicts of Interest: The authors declare no conflict of interest.

References

1. Taylor, J.; Xiao, W.; Abdel-Wahab, O. Diagnosis and classification of hematologic malignancies on the basis of genetics. *Blood* **2017**, *130*, 410–423. [[CrossRef](#)] [[PubMed](#)]
2. Rajkumar, S.V. Multiple myeloma: 2016 update on diagnosis, risk-stratification, and management. *Am. J. Hematol.* **2016**, *91*, 719–734. [[CrossRef](#)] [[PubMed](#)]
3. Juliusson, G.; Hough, R. Leukemia. *Prog. Tumor Res.* **2016**, *43*, 87–100. [[PubMed](#)]
4. Özenver, N.; Dawood, M.; Fleischer, E.; Klinger, A.; Efferth, T. Chemometric and transcriptomic profiling, microtubule disruption and cell death induction by secalononic acid in tumor cells. *Molecules* **2020**, *25*, 3224. [[CrossRef](#)] [[PubMed](#)]
5. Crowell, J.A. The chemopreventive agent development research program in the division of cancer prevention of the US National Cancer Institute: An overview. *Eur. J. Cancer* **2005**, *41*, 1889–1910. [[CrossRef](#)]
6. Maksimović, Z.; Stojanović, D.; Šošćarić, I.; Dajić, Z.; Ristić, M. Composition and radical-scavenging activity of *Thymus glabrescens* wild (Lamiaceae) essential oil. *J. Sci. Food Agric.* **2008**, *88*, 2036–2041.
7. Ahmed, H.M. Ethnopharmacobotanical study on the medicinal plants used by herbalists in Sulaymaniyah Province, Kurdistan, Iraq. *J. Ethnobiol. Ethnomed.* **2016**, *12*, 8. [[CrossRef](#)]
8. Berdowska, I.; Zieliński, B.; Fecka, I.; Kulbacka, J.; Saczko, J.; Gamian, A. Cytotoxic impact of phenolics from Lamiaceae species on human breast cancer cells. *Food Chem.* **2013**, *141*, 1313–1321. [[CrossRef](#)]
9. Nikolić, M.; Glamočlija, J.; Ferreira, I.C.; Calhella, R.C.; Fernandes, Â.; Marković, T.; Marković, D.; Giweli, A.; Soković, M. Chemical composition, antimicrobial, antioxidant and antitumor activity of *Thymus serpyllum* L., *Thymus algeriensis* Boiss. and Reut and *Thymus vulgaris* L. essential oils. *Ind. Crops Prod.* **2014**, *52*, 183–190.
10. Grespan, R.; Aguiar, R.P.; Giubilei, F.N.; Fuso, R.R.; Damião, M.J.; Silva, E.L.; Mikcha, J.G.; Hernandez, L.; Bersani Amado, C.; Cuman, R.K.N. Hepatoprotective effect of pretreatment with *Thymus vulgaris* essential oil in experimental model of acetaminophen-induced injury. *Evid. Based Complement. Alternat. Med.* **2014**, *2014*, 954136.
11. Ayesh, B.M.; Abed, A.A.; Doa'a, M.F. In vitro inhibition of human leukemia THP-1 cells by *Origanum syriacum* L. and *Thymus vulgaris* L. Extracts. *BMC Res. Notes* **2014**, *7*, 612. [[CrossRef](#)]
12. Zu, Y.; Yu, H.; Liang, L.; Fu, Y.; Efferth, T.; Liu, X.; Wu, N. Activities of ten essential oils towards *Propionibacterium acnes* and PC-3, A-549 and MCF-7 cancer cells. *Molecules* **2010**, *15*, 3200–3210. [[CrossRef](#)] [[PubMed](#)]
13. Al-Menhali, A.; Al-Rumaihi, A.; Al-Mohammed, H.; Al-Mazrooey, H.; Al-Shamlan, M.; AlJassim, M.; Al-Korbi, N.; Eid, A.H. *Thymus vulgaris* (thyme) inhibits proliferation, adhesion, migration, and invasion of human colorectal cancer cells. *J. Med. Food* **2015**, *18*, 54–59. [[CrossRef](#)]
14. Ahmad, S.A.; Askari, A.A. Ethnobotany of the Hawraman region of Kurdistan Iraq. *Harv. Pap. Bot.* **2015**, *20*, 85–89. [[CrossRef](#)]
15. JianFeng, C.; PengYing, Z.; ChengWei, X.; TaoTao, H.; YunGui, B.; KaoShan, C. Effect of aqueous extract of *Arctium lappa* L. (burdock) roots on the sexual behavior of male rats. *BMC Complement. Altern. Med.* **2012**, *12*, 8. [[CrossRef](#)]
16. Badarau, A.S.; Wang, D.; Swamy, M.K.; Shaw, S.; Maggi, F.; Da Silva, L.E.; López, V.; Yeung, A.W.K.; Mocan, A.; Atanasov, A.G. *Arctium* species secondary metabolites chemodiversity and bioactivities. *Front. Plant Sci.* **2019**, *10*, 834.
17. Lou, C.; Zhu, Z.; Zhao, Y.; Zhu, R.; Zhao, H. Arctigenin, a lignan from *Arctium lappa* L., inhibits metastasis of human breast cancer cells through the downregulation of MMP-2/-9 and heparanase in MDA-MB-231 cells. *Oncol. Rep.* **2017**, *37*, 179–184. [[CrossRef](#)] [[PubMed](#)]
18. Tian, X.; Guo, L.-P.; Hu, X.-L.; Huang, J.; Fan, Y.-H.; Ren, T.-S.; Zhao, Q.-C. Protective effects of *Arctium lappa* L. roots against hydrogen peroxide-induced cell injury and potential mechanisms in SH-SY5Y cells. *Cell. Mol. Neurobiol.* **2015**, *35*, 335–344. [[CrossRef](#)] [[PubMed](#)]
19. Predes, F.S.; Ruiz, A.L.; Carvalho, J.E.; Foglio, M.A.; Dolder, H. Antioxidative and in vitro antiproliferative activity of *Arctium lappa* root extracts. *BMC Complement Altern. Med.* **2011**, *11*, 25.
20. Naqishbandi, A. Plants used in Iraqi traditional medicine in Erbil-Kurdistan region. *Zanco J. Med. Sci.* **2014**, *18*, 811–815. [[CrossRef](#)]

21. Efferth, T.; Konkimalla, V.B.; Wang, Y.-F.; Sauerbrey, A.; Meinhardt, S.; Zintl, F.; Mattern, J.; Volm, M. Prediction of broad spectrum resistance of tumors towards anticancer drugs. *Clin. Cancer Res.* **2008**, *14*, 2405–2412. [[CrossRef](#)] [[PubMed](#)]
22. Mbaveng, A.T.; Damen, F.; Simo Mpetga, J.D.; Awouafack, M.D.; Tane, P.; Kuete, V.; Efferth, T. Cytotoxicity of crude extract and isolated constituents of the *Dichrostachys cinerea* bark towards multifactorial drug-resistant cancer cells. *Evid. Based Complement. Alternat. Med.* **2019**, *2019*, 8450158. [[CrossRef](#)] [[PubMed](#)]
23. Mothana, R.A.; Lindequist, U.; Gruenert, R.; Bednarski, P.J. Studies of the in vitro anticancer, antimicrobial and antioxidant potentials of selected Yemeni medicinal plants from the island Soqatra. *BMC Complement Altern. Med.* **2009**, *9*, 7. [[CrossRef](#)]
24. Radovanovic, A. Evaluation of potential cytotoxic effects of herbal extracts. *Serbian J. Exp. Clin. Res.* **2015**, *16*, 333–342. [[CrossRef](#)]
25. Turner, J.G.; Dawson, J.L.; Grant, S.; Shain, K.H.; Dalton, W.S.; Dai, Y.; Meads, M.; Baz, R.; Kauffman, M.; Shacham, S. Treatment of acquired drug resistance in multiple myeloma by combination therapy with XPO1 and topoisomerase II inhibitors. *J. Hematol. Oncol.* **2016**, *9*, 1–11. [[CrossRef](#)]
26. Pereyra, C.E.; Dantas, R.F.; Ferreira, S.B.; Gomes, L.P.; Silva-Jr, F.P. The diverse mechanisms and anticancer potential of naphthoquinones. *Cancer Cell Int.* **2019**, *19*, 1–20. [[CrossRef](#)]
27. Pacifico, S.; Piccolella, S.; Papale, F.; Nocera, P.; Lettieri, A.; Catauro, M. A polyphenol complex from *Thymus vulgaris* L. plants cultivated in the Campania Region (Italy): New perspectives against neuroblastoma. *J. Funct. Foods* **2016**, *20*, 253–266. [[CrossRef](#)]
28. Al-seragy, I.M.; Kharat, K.R.; Dhabe, A.S. Cell cycle arrest and induction of apoptosis in human breast cancer cells (T-47D) by *Annona squamosa* L. and *Thymus vulgaris* L. ethanolic extract. *J. Biol. Active Prod. Nat.* **2019**, *9*, 47–56. [[CrossRef](#)]
29. Don, R.A.S.G.; Yap, M.K.K. *Arctium lappa* L. root extract induces cell death via mitochondrial-mediated caspase-dependent apoptosis in Jurkat human leukemic T cells. *Biomed. Pharmacother.* **2019**, *110*, 918–929.
30. Jeong, J.B.; Hong, S.C.; Jeong, H.J.; Koo, J.S. Arctigenin induces cell cycle arrest by blocking the phosphorylation of Rb via the modulation of cell cycle regulatory proteins in human gastric cancer cells. *Int. Immunopharmacol.* **2011**, *11*, 1573–1577. [[CrossRef](#)]
31. Yan, G.; Elbadawi, M.; Efferth, T. Multiple cell death modalities and their key features. *World Acad. Sci. J.* **2020**, *2*, 39–48. [[CrossRef](#)]
32. Dixon, S.J. Ferroptosis: Bug or feature? *Immunol. Rev.* **2017**, *277*, 150–157. [[CrossRef](#)]
33. Ooko, E.; Saeed, M.E.; Kadioglu, O.; Sarvi, S.; Colak, M.; Elmasaoudi, K.; Janah, R.; Greten, H.J.; Efferth, T. Artemisinin derivatives induce iron-dependent cell death (ferroptosis) in tumor cells. *Phytomedicine* **2015**, *22*, 1045–1054. [[CrossRef](#)]
34. Park, J.M.; Tougeron, D.; Huang, S.; Okamoto, K.; Sinicrope, F.A. Beclin 1 and UVRAG confer protection from radiation-induced DNA damage and maintain centrosome stability in colorectal cancer cells. *PLoS ONE* **2014**, *9*, e100819.
35. Kabeya, Y.; Mizushima, N.; Ueno, T.; Yamamoto, A.; Kirisako, T.; Noda, T.; Kominami, E.; Ohsumi, Y.; Yoshimori, T. LC3, a mammalian homologue of yeast Apg8p, is localized in autophagosome membranes after processing. *EMBO J.* **2000**, *19*, 5720–5728. [[CrossRef](#)]
36. Barreca, D.; Mandalari, G.; Calderaro, A.; Smeriglio, A.; Trombetta, D.; Felice, M.R.; Gattuso, G. Citrus flavones: An update on sources, biological functions, and health promoting properties. *Plants* **2020**, *9*, 288. [[CrossRef](#)]
37. Adham, A.N.; Abdelfatah, S.; Naqishbandi, A.M.; Mahmoud, N.; Efferth, T. Cytotoxicity of apigenin toward multiple myeloma cell lines and suppression of iNOS and COX-2 expression in STAT1-transfected HEK293 cells. *Phytomedicine* **2020**, *80*, 153371. [[CrossRef](#)]
38. Zhang, L.; Cheng, X.; Gao, Y.; Zheng, J.; Xu, Q.; Sun, Y.; Guan, H.; Yu, H.; Sun, Z. Apigenin induces autophagic cell death in human papillary thyroid carcinoma BCPAP cells. *Food Funct.* **2015**, *6*, 3464–3472. [[CrossRef](#)]
39. Yoshimizu, N.; Otani, Y.; Saikawa, Y.; Kubota, T.; Yoshida, M.; Furukawa, T.; Kumai, K.; Kameyama, K.; Fujii, M.; Yano, M. Anti-tumour effects of nobiletin, a citrus flavonoid, on gastric cancer include: Antiproliferative effects, induction of apoptosis and cell cycle deregulation. *Aliment. Pharmacol. Ther.* **2004**, *20*, 95–101. [[CrossRef](#)]

40. Ikeda, A.; Nemoto, K.; Yoshida, C.; Miyata, S.; Mori, J.; Soejima, S.; Yokosuka, A.; Mimaki, Y.; Ohizumi, Y.; Degawa, M. Suppressive effect of nobiletin, a citrus polymethoxyflavonoid that downregulates thioredoxin-interacting protein expression, on tunicamycin-induced apoptosis in SK-N-SH human neuroblastoma cells. *Neurosci. Lett.* **2013**, *549*, 135–139. [[CrossRef](#)]
41. Wang, J.-S.; Ren, T.-N.; Xi, T. Ursolic acid induces apoptosis by suppressing the expression of FoxM1 in MCF-7 human breast cancer cells. *Med. Oncol.* **2012**, *29*, 10–15. [[CrossRef](#)]
42. Kim, K.H.; Seo, H.S.; Choi, H.S.; Choi, I.; Shin, Y.C.; Ko, S.-G. Induction of apoptotic cell death by ursolic acid through mitochondrial death pathway and extrinsic death receptor pathway in MDA-MB-231 cells. *Arch. Pharmacol. Res.* **2011**, *34*, 1363. [[CrossRef](#)] [[PubMed](#)]
43. Shen, S.; Zhang, Y.; Zhang, R.; Tu, X.; Gong, X. Ursolic acid induces autophagy in U87MG cells via ROS-dependent endoplasmic reticulum stress. *Chem. Biol. Interact.* **2014**, *218*, 28–41. [[CrossRef](#)] [[PubMed](#)]
44. Cmoch, P.; Pakulski, Z.; Swaczynová, J.; Strnad, M. Synthesis of lupane-type saponins bearing mannosyl and 3, 6-branched trimannosyl residues and their evaluation as anticancer agents. *Carbohydr. Res.* **2008**, *343*, 995–1003. [[CrossRef](#)]
45. Aratanechemuge, Y.; Hibasami, H.; Sanpin, K.; Katsuzaki, H.; Imai, K.; Komiya, T. Induction of apoptosis by lupeol isolated from mokumen (*Gossampinus malabarica* L. Merr) in human promyelotic leukemia HL-60 cells. *Oncol. Rep.* **2004**, *11*, 289–292. [[CrossRef](#)]
46. Redfern, J.; Kinninmonth, M.; Burdass, D.; Verran, J. Using soxhlet ethanol extraction to produce and test plant material (essential oils) for their antimicrobial properties. *J. Microbiol. Biol. Educ.* **2014**, *15*, 45. [[CrossRef](#)]
47. Leich, E.; Weissbach, S.; Klein, H.; Grieb, T.; Pischmarov, J.; Stühmer, T.; Chatterjee, M.; Steinbrunn, T.; Langer, C.; Eilers, M. Multiple myeloma is affected by multiple and heterogeneous somatic mutations in adhesion-and receptor tyrosine kinase signaling molecules. *Blood Cancer J.* **2013**, *3*, e102. [[CrossRef](#)]
48. Efferth, T.; Sauerbrey, A.; Olbrich, A.; Gebhart, E.; Rauch, P.; Weber, H.O.; Hengstler, J.G.; Halatsch, M.-E.; Volm, M.; Tew, K.D. Molecular modes of action of artesunate in tumor cell lines. *Mol. Pharmacol.* **2003**, *64*, 382–394. [[CrossRef](#)]
49. Özenver, N.; Saeed, M.; Demirezer, L.Ö.; Efferth, T. Aloe-emodin as drug candidate for cancer therapy. *Oncotarget* **2018**, *9*, 17770. [[CrossRef](#)]
50. Hegazy, M.-E.F.; Abdelfatah, S.; Hamed, A.R.; Mohamed, T.A.; Elshamy, A.A.; Saleh, I.A.; Reda, E.H.; Abdel-Azim, N.S.; Shams, K.A.; Sakr, M. Cytotoxicity of 40 Egyptian plant extracts targeting mechanisms of drug-resistant cancer cells. *Phytomedicine* **2019**, *59*, 152771. [[CrossRef](#)]
51. Mbaveng, A.T.; Bitchagno, G.T.; Kuete, V.; Tane, P.; Efferth, T. Cytotoxicity of ungeremine towards multi-factorial drug resistant cancer cells and induction of apoptosis, ferroptosis, necroptosis and autophagy. *Phytomedicine* **2019**, *60*, 152832. [[CrossRef](#)]
52. Abdelfatah, S.; Böckers, M.; Asensio, M.; Kadioglu, O.; Klinger, A.; Fleischer, E.; Efferth, T. Isopetasin and S-isopetasin as novel P-glycoprotein inhibitors against multidrug-resistant cancer cells. *Phytomedicine* **2020**, 153196. [[CrossRef](#)]
53. Kuete, V.; Mbaveng, A.T.; Sandjo, L.P.; Zeino, M.; Efferth, T. Cytotoxicity and mode of action of a naturally occurring naphthoquinone, 2-acetyl-7-methoxynaphtho [2, 3-b] furan-4, 9-quinone towards multi-factorial drug-resistant cancer cells. *Phytomedicine* **2017**, *33*, 62–68. [[CrossRef](#)]
54. Mbaveng, A.T.; Fotso, G.W.; Ngnintedo, D.; Kuete, V.; Ngadjui, B.T.; Keumedjio, F.; Andrae-Marobela, K.; Efferth, T. Cytotoxicity of epunctanone and four other phytochemicals isolated from the medicinal plants *Garcinia epunctata* and *Ptycholobium contortum* towards multi-factorial drug resistant cancer cells. *Phytomedicine* **2018**, *48*, 112–119. [[CrossRef](#)]
55. Adem, F.A.; Mbaveng, A.T.; Kuete, V.; Heydenreich, M.; Ndakala, A.; Irungu, B.; Yenesew, A.; Efferth, T. Cytotoxicity of isoflavones and biflavonoids from *Ormocarpum kirkii* towards multi-factorial drug resistant cancer. *Phytomedicine* **2019**, *58*, 152853. [[CrossRef](#)]
56. Nakata, S.; Yoshida, T.; Horinaka, M.; Shiraiishi, T.; Wakada, M.; Sakai, T. Histone deacetylase inhibitors upregulate death receptor 5/TRAIL-R2 and sensitize apoptosis induced by TRAIL/APO2-L in human malignant tumor cells. *Oncogene* **2004**, *23*, 6261–6271. [[CrossRef](#)]

57. Papi, A.; Farabegoli, F.; Iori, R.; Orlandi, M.; De Nicola, G.R.; Bagatta, M.; Angelino, D.; Gennari, L.; Ninfali, P. Vitexin-2-O-xyloside, raphasatin and (–)-epigallocatechin-3-gallate synergistically affect cell growth and apoptosis of colon cancer cells. *Food Chem.* **2013**, *138*, 1521–1530. [[CrossRef](#)]
58. Zhao, Q.; Kretschmer, N.; Bauer, R.; Efferth, T. Shikonin and its derivatives inhibit the epidermal growth factor receptor signaling and synergistically kill glioblastoma cells in combination with erlotinib. *Int. J. Cancer* **2015**, *137*, 1446–1456. [[CrossRef](#)]

Sample Availability: All samples of the compounds are available from the authors.

Publisher’s Note: MDPI stays neutral with regard to jurisdictional claims in published maps and institutional affiliations.



© 2020 by the authors. Licensee MDPI, Basel, Switzerland. This article is an open access article distributed under the terms and conditions of the Creative Commons Attribution (CC BY) license (<http://creativecommons.org/licenses/by/4.0/>).